A wake detector for wind farm control

A wake detector for wind farm control

C L Bottasso[1,2]**, S Cacciola**[1] **and J Schreiber**[1]
[1] Technische Universität München, München, Germany
[2] Politecnico di Milano, Milano, Italy

E-mail: carlo.bottasso@tum.de

Abstract. The paper describes an observer capable of detecting the impingement on a wind turbine rotor of the wake of an upstream machine. The observer estimates the local wind speed and turbulence intensity on the left and right parts of the rotor disk. The estimation is performed based on blade loads measured by strain gages or optical fibers, sensors which are becoming standard equipment on many modern machines. A lower wind speed and higher turbulence intensity on one part of the rotor, possibly in conjunction with other information, can then be used to infer the presence of a wake impinging on the disk. The wake state information is useful for wind plant control strategies, as for example wake deflection by active yawing. In addition, the local wind speed estimates may be used for a rough evaluation of the vertical wind shear.

1. Introduction and motivation

Wind turbines operating in a wind plant may be affected by the wake of neighboring wind turbines. When this happens, the affected machine experiences reduced power output and increased fatigue loading. The problem of how to control the machines within a wind power plant to minimize the undesirable effects of wake interactions is nowadays the subject of intensive research [1-3], enabled by the development of suitable wake models [3,4].

The implementation of control strategies to address this problem may require the ability to detect such an interference condition. For example, figure 1 depicts the case of wind plant control by wake deflection; in such a case, the detection of a wake interference condition may be used to yaw the affecting wind turbine until a clean condition on the affected machine is achieved.

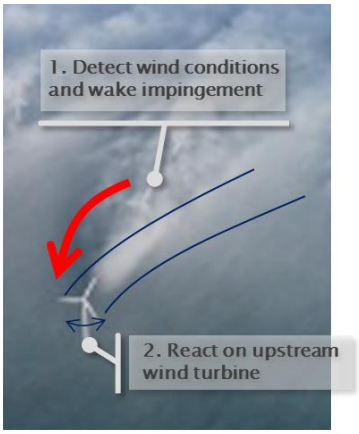

Figure 1. Wake interference detection followed by deflection.

This paper describes a methodology to detect wake impingement on a wind turbine caused by an upstream machine. LiDARs (Light Detection and Ranging) may be able to detect the location of a wind turbine wake [5], and therefore in principle they could be used to achieve such a goal. However, their use is still confined to research applications, and they are not yet routinely deployed in the field on production machines. In this work, the wake interference detection is based on the use of rotor loads. In fact, as rotor load sensors are becoming commonly available on modern wind turbines, for example to enable individual blade pitch control, no additional sensors or equipment are necessary for the implementation of the present method. The use of rotor loads for the detection of wind conditions is a technology that has been proposed and demonstrated in [6-10]. The present work extends the technology to the estimation of the wake state.

The proposed method is based on the estimation of the wind speed by the out-of-plane blade root bending moment. Similarly to the thrust coefficient, a cone root bending coefficient may be defined, which depends on the tip speed ratio and blade pitch. Using the three blades together, knowledge of the loads in addition to rotor speed and blade pitch setting allows one to estimate from the cone coefficient a rotor-equivalent wind speed. On the other hand, when using the information for each single blade, one may sense the wind at the azimuthal location occupied by that blade. Averaging over an azimuthal interval, an estimate of the local wind speed in a rotor sector can be readily obtained, from which in turn one may also obtain an estimate of the turbulence intensity.

2. Methods

At first, a new rotor-effective wind speed estimator is developed, based on the out-of-plane cone (i.e. averaged over the number of blades) bending rotor loads. The cone coefficient is defined as

$$C_{m_0}(\lambda_{RE},\beta,V_{RE}) = \frac{\frac{1}{2\pi}\int_{\psi=0}^{2\pi}\sum_{i=1}^{B} m_i(\psi_i)\,\mathrm{d}\psi}{\frac{1}{2}\rho A R {V_{RE}}^2}, \tag{1}$$

where λ_{RE} is the rotor-effective tip speed ratio, β the pitch angle, m_i the out-of-plane bending moment of blade i, which occupies the azimuthal position ψ_i, ρ is the density of air, A the rotor disc area, R the rotor radius and V_{RE} the unknown rotor-effective wind speed. This latter quantity can be now interpreted as that constant wind speed that induces the same out-of-plane bending moment as the one being currently measured. With this definition, the blade collective bending moment (per blade) $m_0 = \sum_{i=1}^{B} m_i/B$ is computed as

$$m_0(t) = \frac{1}{2B}\rho A R\, {V_{RE}}^2(t)\, C_{m_0}\big(\lambda_{RE}(t),\beta(t),V_{RE}(t)\big), \tag{2}$$

where B is the number of blades. At each instant of time, m_0 is measured by blade load sensors. As also the rotor speed Ω can be easily measured together with the blade pitch angle β, the sole unknown in the equation is the effective wind speed V_{RE}, which can therefore be readily computed.

To increase robustness of the estimates in the face of measurement and process noise, an Extended Kalman filter is used for the computation of V_{RE}. The wind speed update is defined as

$$V_{RE_k} = V_{RE_{k-1}} + w_{k-1}, \tag{3}$$

w_k being the process noise with covariance $\boldsymbol{Q}$, while the non-linear output equation is defined as

$$z_k = \frac{1}{2}\rho A R\, {V_{RE}}_k^2\, C_{m0}(\lambda_{RE},\beta) - \hat{m}_0 + v_k, \tag{4}$$

where v_k is the measurement noise with covariance $\boldsymbol{R}$, $\hat{m}_0$ are the measured loads, while the output z_k is set to 0 to enforce the desired equation at each step.

Such a method delivers estimates of the wind speed and turbulence intensity that are similar, if not slightly superior, to the classical rotor-effective wind speed estimators based on the torque balance equation using the power coefficient C_P [11]. In fact, the present approach may be somewhat less limited in frequency than the classical one, which is slowed by the significant inertia of the rotor. An example of the quality of the resulting estimates of the wind speed in the time domain is shown in figure 2. The effective wind speed reference, shown in the figure using a black solid line, was computed from the simulation input as the spatial mean of the longitudinal wind speed within the rotor disk area, as already done in Østergaard et al. [12].

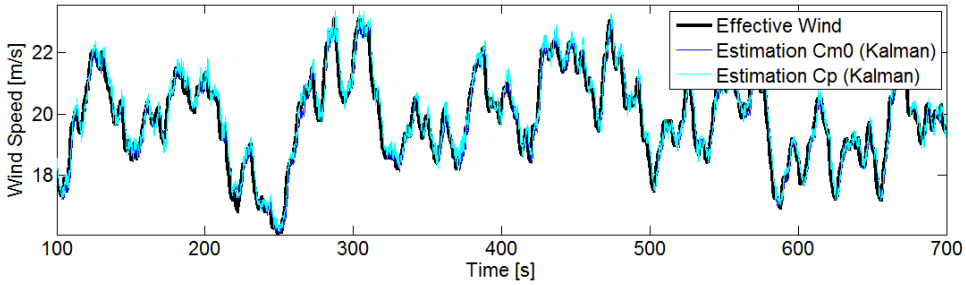

Figure 2. Effective wind speed time history, and its estimates obtained by the cone estimator using the C_{m_0} coefficient, or the classical formulation based on the power coefficient C_P [11].

The estimates provided by the present method are of good accuracy and robustness with respect to the tuning parameters of the filter, as shown in figure 3.

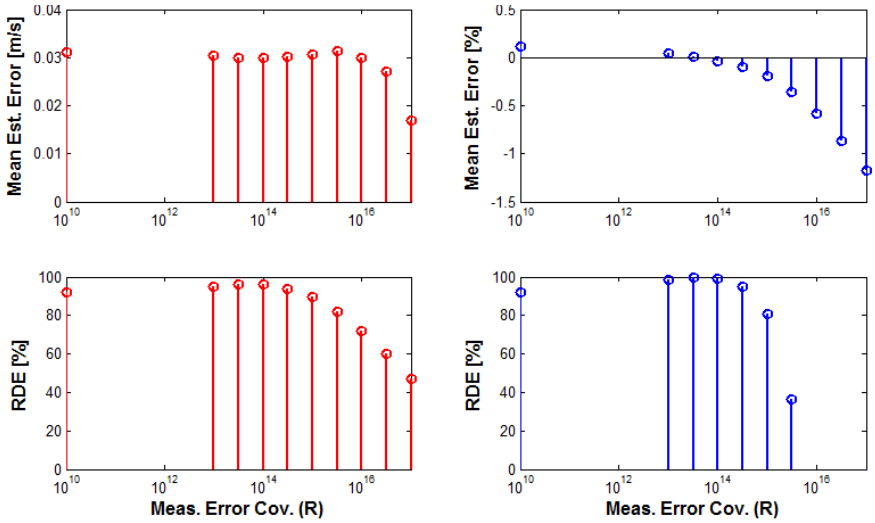

Figure 3. Estimation of rotor-effective wind speed (left) and turbulence intensity (right): mean estimation error (top), and relative degree of explanation (RDE) [11] (bottom).

Next, the method is specialized to the estimation of wind speed on sectors of the rotor disk. To this end, considering the *i*th blade, the previous moment equation is modified as

$$m_i(t) = \frac{1}{2B}\rho A R\, {V_{LE}}^2(t,\psi)\, C_{m_0}\big(\lambda_{LE}(t,\psi), \beta(t), V_{LE}(t)\big), \tag{5}$$

where the blade local-effective wind speed is defined as

$$V_{LE}(\psi) = \frac{1}{A_B}\int_{A_B} V \mathrm{d}A_B(\psi), \tag{6}$$

A_B being the planform area of the rotor blade. As clear from (6), the *i*th blade local-effective wind speed can be seen as that constant wind speed that would lead to the same out-of-plane-bending moment of the *i*th blade. From the blade local-effective wind speed, a sector-effective wind speed is obtained by averaging over an azimuthal interval of interest. The concept is illustrated in figure 4, which shows how the passage of a blade over a disk sector can be used for estimating a sector-effective wind speed:

$$V_{SE}(\tilde{t}) = \frac{1}{A_S}\int_{A_S} V_{LE}(t,\psi)\, \mathrm{d}A_S = \frac{1}{\psi_2 - \psi_1}\int_{\psi_1}^{\psi_2} V_{LE}(t,\psi)\mathrm{d}\psi. \tag{7}$$

Finally, from the knowledge of the wind speed, the sector turbulence intensity can be readily computed.

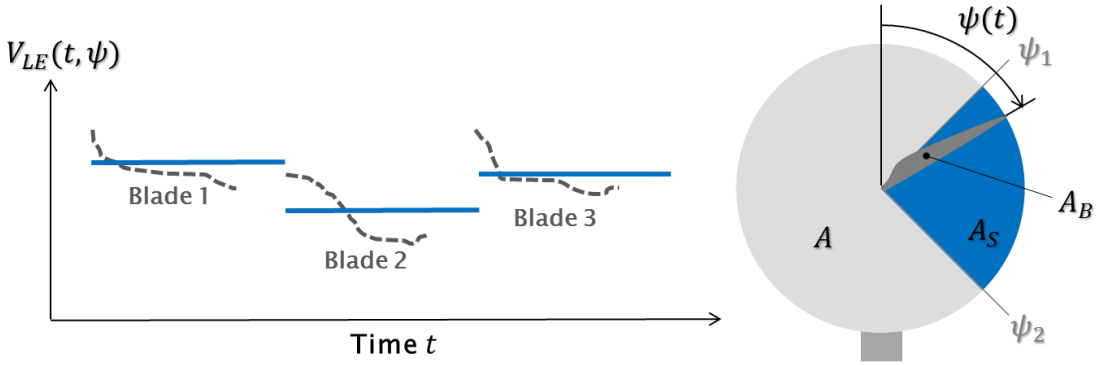

Figure 4. Estimation of local-effective and sector-effective wind speed and turbulence intensity, from the loads of a blade passing through a rotor disk sector.

3. Results

At first, the new method was tested using field data of the NREL CART 3 wind turbine [13]. As no known wake interference condition of that machine with other wind turbines was available for this study, the local wind estimation method was used to estimate the different velocities in the top and bottom quadrants of the rotor, which gives an idea of the vertical wind shear.

Using a nearby met-mast, a comparison with anemometer measurements can be performed, the position of the anemometers being shown in figure 5. To compare with these two point measurements, it is useful to derive a point measurement from the sector-effective wind speed estimated by the present method. To this end, the blade bending moment averaged over the sector, m_{iS}, can be alternatively computed as

$$m_{iS} = \frac{1}{2B}\rho \int_{\psi_1}^{\psi_2}\int_0^R V^2(\psi,r)\, C_T(\psi,r) r^2 \mathrm{d}r\, \mathrm{d}\psi, \tag{7}$$

where C_T is the local thrust coefficient. Assuming a constant speed and thrust coefficient over the rotor disk, the bending moment is readily expressed as

$$m_{iS} = \frac{1}{2B}\rho A_S V_{SE}^2 C_T \frac{2}{3} R. \tag{8}$$

This expression shows that the bending loads used for estimating the sector-effective wind speed can be seen as generated by the sector thrust applied at $2/3\ R$; in this sense, the estimator can be interpreted as sampling the wind field at about 66% of the blade span. Consequently, the anemometer measurements were interpolated at hub height $\pm 2/3\ R$ and used as reference measurements in the following plot to judge the quality of the load-based estimates.

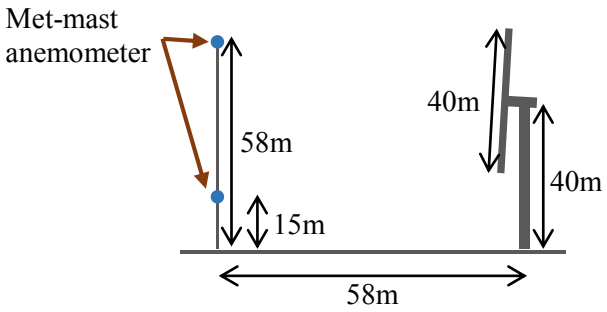

Figure 5. Sketch of met-mast anemometer position wrt the NREL CART 3 wind turbine.

Figure 6 shows a good agreement between the estimated sector-effective wind speeds with the interpolated point-wise anemometer measurements. The trends are reasonably well followed and a higher wind speed is detected in the top than in the bottom quadrant.

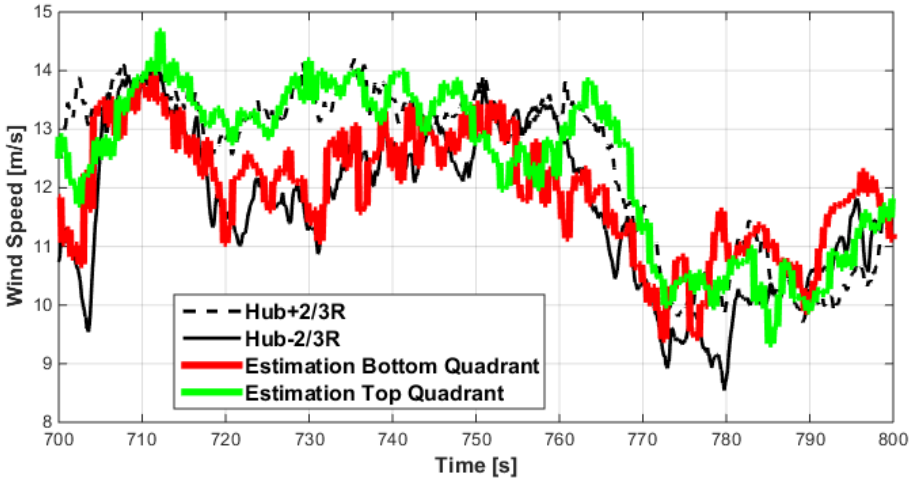

Figure 6. Estimation of top and bottom quadrant effective wind speeds, and comparison with interpolated met-mast data for the NREL CART 3 wind turbine.

Finally, the new method was used for estimating the local wind speed separately on the left and right parts of the rotor, thereby detecting the possible presence of an area of reduced speed and increased turbulence intensity, which may indicate the presence of a wake. As no experimental data was available

for this case, a simulation study was conducted, by using a high-fidelity aeroservoelastic model [14] of a multi-MW wind turbine operating in different partial and full wake conditions. A representative image of the wind field at the rotor disk in waked and unwaked conditions is shown if figure 7.

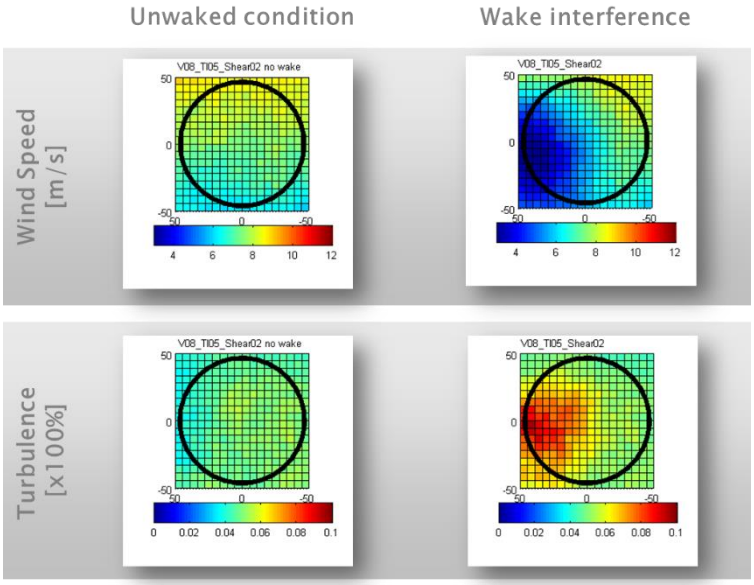

Figure 7. Wind field at the rotor disk in unwaked (left) and waked (right) conditions.

The results of the estimation are summarized by figures 8 and 9, which show the actual and estimated local wind speeds and turbulence intensities in two lateral quadrants of the rotor. Each subplot refers to a different overlap indicated by the lateral distance between the rotor and the wake center.

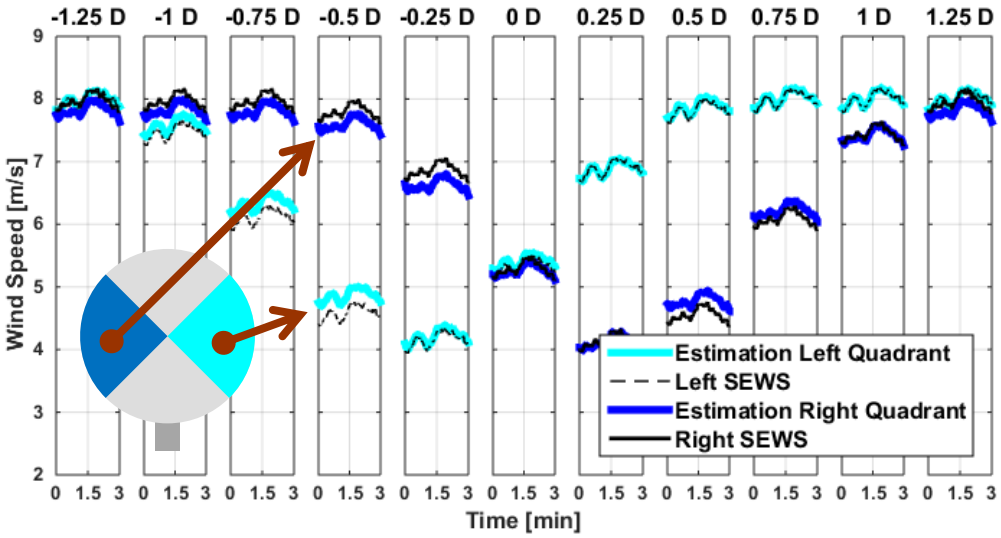

Figure 8. Estimation of local wind speed on two lateral rotor quadrants.

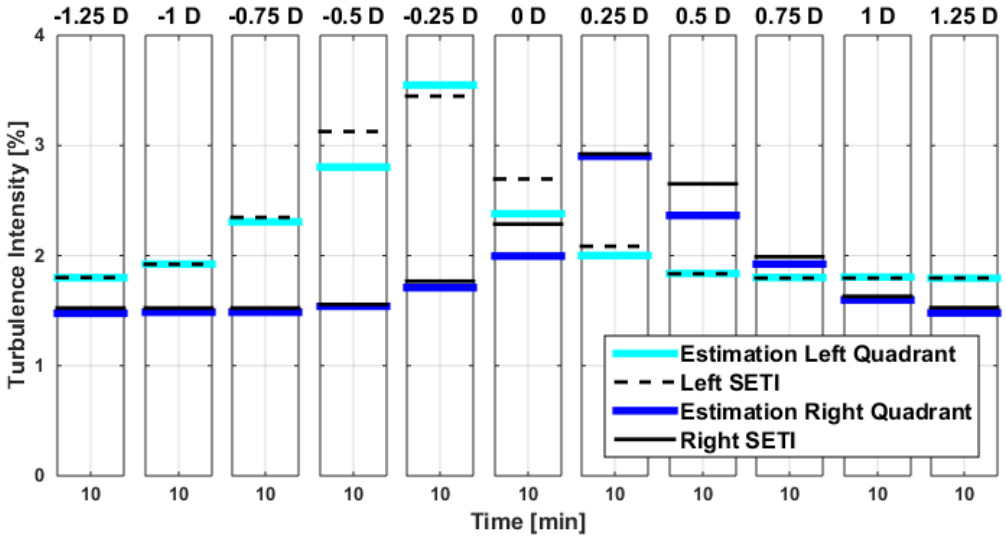

Figure 9. Estimation of local wind turbulence intensity on two lateral rotor quadrants.

4. Conclusions

As well illustrated by the results shown here, the proposed method is capable of estimating with good accuracy the local wind speed and turbulence intensity, and in particular it is able to detect variations of these quantities on the two sides of the rotor that may be indicative of a wake interference condition. Similar results can be derived for various wind conditions, demonstrating the robustness of the local wind speed estimator. The new wake detector is currently being used for driving wake deflection strategies by active wind turbine yaw. In addition, the same approach may be used for a rough estimation of the vertical wind shear.

References

[1] Lund B F, Oma P N and Jakobsen T 2014 Wind farm production maximization through joint optimization of turbine efficiency and yaw. Simulated case studies. *Poster EWEA* (Barcelona, Spain)

[2] Park J, Kwon S and Law K H 2013 Wind farm power maximization based on a cooperative static game approach *Proceedings of the SPIE Active and Passive Smart Structures and Integrated Systems Conference* (San Diego, USA)

[3] Fleming P, Gebraad P, Lee S, van Wingerden J, Johnson K, Churchfield M, Michalakes J, Spalart P, Moriarty P 2013 High-fidelity simulation comparison of wake mitigation control strategies for a two-turbine case *Proceedings of ICOWES Conference* (Lyngby, Denmark)

[4] Hao Y, Lackner M, Keck R E, Lee S, Churchfield M, Moriarty P 2013 Implementing the dynamic wake meandering model in the NWTC design codes *AIAA*

[5] Bingöl F, Mann J, Larsen G. 2010 Light detection and ranging measurements of wake dynamics. Part I: one-dimensional scanning. *Wind Energy* **13** 51–61

[6] Bottasso C L and Riboldi C E D 2015 Validation of a wind misalignment observer using field test data *Renewable Energy* **74** 298–306

[7] Bottasso C L and Riboldi C E D 2014 Estimation of wind misalignment and vertical shear from blade loads *Renewable Energy* **62** 293–302

[8] Bottasso C L, Campagnolo F and Petrović V 2014 Wind tunnel testing of scaled wind turbine models: beyond aerodynamics *J Wind Eng Ind Aerod* **127** 11–28

[9] Bottasso C L, Croce A and Riboldi C E D 2010 Spatial estimation of wind states from the aeroelastic response of a wind turbine *Proc. TORQUE* (Heraklion, Greece)

[10] Bottasso C L, Croce A, Riboldi C E D and Bir G 2009 Real-time estimation of structural and wind states for wind turbine advanced control *Proc. EWEC* (Marseille, France)
[11] Soltani M and Wisniewsky R 2013 Estimation of rotor effective wind speed: a comparison *IEEE Trans. Contr. Syst. Technol.* **21**(4) 1155–1167
[12] Østergaard KZ, Brath P, Stoustrup J 2007 Estimation of effective wind speed *Journal of Physics: Conference Series 75, EWEA*
[13] Fleming P A, Wright A D, Fingersh L J and van Wingerden J W 2011 Resonant vibrations resulting from the re-engineering of a constant-speed 2-bladed turbine to a variable-speed 3-bladed turbine *Proc. 49th AIAA Aerospace Sciences Meeting* (Orlando, Florida)
[14] Bottasso C L and Croce A 2006–2015 *Cp-Lambda – User's Manual* Politecnico di Milano (Milano, Italy)